buildings

MDPI

Article

Improving the Thermochemical Heat Storage Performance of Calcium Hydroxide in a Fixed-Bed Reactor by Y-Shaped Fins

Guangyao Zhao [1,2], Zhen Li [1,2,*], Jiakang Yao [1,2], Zhehui Zhao [1,2], Sixing Zhang [1,2], Na Cheng [1,2], Lei Jiang [3] and Jun Yan [3,*]

[1] State Key Laboratory of Advanced Power Transmission Technology, Beijing 100192, China; zhaoguangyao@epri.sgcc.com.cn (G.Z.)
[2] China Electric Power Research Institute, Beijing 100192, China
[3] Institute of Engineering Thermophysics, School of Mechanical Engineering, Shanghai Jiao Tong University, Shanghai 200240, China
* Correspondence: lzh1@epri.sgcc.com.cn (Z.L.); miraclebwh@sjtu.edu.cn (J.Y.)

Abstract: Thermochemical heat storage technology has great development prospects due to its high energy storage density and stable long-term storage capacity. The calcium hydroxide/calcium oxide reaction has been proven to be feasible for thermochemical heat storage. However, due to its low thermal conductivity, the slow heat storage reaction in the fixed-bed reactor needs to be improved. In this work, the Y-shaped fin was used to improve the heat storage performance, and a multi-physics numerical model was established for its heat storage process in the fixed bed. The results show that the Y-shaped fin can accelerate the heat storage reaction due to the improved heat transfer inside the reactor. The heat storage time decreases by 45.59% compared to the reactor without a fin and it decreases by 4.31% compared to the reactor with the rectangular fin. The increase in the wall temperature of the heating tube and the thermal conductivity of the fin can improve the heat storage performance; moreover, the Y-shaped fin shows more performance improvement than the rectangular fin at high wall temperature or thermal conductivity. The increase in porosity of heat storage material can shorten heat storage time due to the reduction in reactant, and the Y-shaped fin can still give a better performance than the rectangular fin at different porosity levels. This work can provide a reference for improving the heat storage performance of fixed-bed reactors.

Keywords: thermochemical heat storage; calcium hydroxide; fixed bed; Y-shaped fin; heat storage performance

Citation: Zhao, G.; Li, Z.; Yao, J.; Zhao, Z.; Zhang, S.; Cheng, N.; Jiang, L.; Yan, J. Improving the Thermochemical Heat Storage Performance of Calcium Hydroxide in a Fixed-Bed Reactor by Y-Shaped Fins. *Buildings* **2024**, *14*, 3694. https://doi.org/10.3390/buildings14113694

Academic Editors: Chi Yan Tso and Jianheng Chen

Received: 25 September 2024
Revised: 11 November 2024
Accepted: 18 November 2024
Published: 20 November 2024

1. Introduction

With the continuous growth in industrialization and excessive dependence on traditional fossil fuels, the accompanying environmental problems become more and more serious, which urgently requires adjusting the existing energy structure [1,2]. Developing renewable energy resources such as solar energy, wind energy, and geothermal energy is an alternative approach to address these issues. However, most renewable energy resources suffer from fluctuations, uniform spatial and temporal distribution, and supply–demand mismatch, which have become obstacles to their current utilization. Energy storage technology is regarded as a viable path to dealing with these issues of renewable energy [3,4]. The energy utilization efficiency can be improved by integrating energy storage components into renewable energy systems [5,6]. Considering that thermal energy occurs in most energy utilization processes, it is necessary to develop thermal energy storage technology [7]. Currently, there are three main types of thermal energy storage: sensible heat storage, latent heat storage, and thermochemical heat storage. Among them, thermochemical heat storage has broad development prospects due to its advantages of high energy storage density, spatial transferability, and stable long-term storage capacity [8,9]. There are many materials that can be used for thermochemical heat storage, for example, metal hydrides

(MgH_2/Mg), metal hydroxides ($Ca(OH)_2$/CaO and $Mg(OH)_2$/MgO), metallic carbonates ($CaCO_3$/CaO and $MgCO_3$/MgO), and metal oxides (Co_3O_4/CoO, Mn_3O_4/Mn_2O_3, and Cu_2O/CuO). The $Ca(OH)_2$/CaO reversible reaction, which works on the basis of Equation (1), has received much attention in recent years [10,11]. It can offer a high energy storage density (1411 kJ/kg) in the medium and high-temperature range (over 400 °C). Moreover, it also has the advantages of low cost, non-toxic, low pollution, and corrosiveness [12,13]. Therefore, it has significant development value.

$$Ca(OH)_2 + \Delta H \Leftrightarrow CaO + H_2O \; \Delta H = 104.4 \text{ kJ/mol} \quad (1)$$

Nevertheless, the slow heat storage process inside the reactor hinders its application, which is mainly due to the low thermal conductivity of heat storage material. The $Ca(OH)_2$/CaO is a gas–solid reaction, and its reaction process is related to temperature and pressure. The reversible reaction rate is controlled by the equilibrium temperature and pressure [14]. That is to say, the heat storage reaction rate becomes slow when the actual temperature is close to the equilibrium temperature. Hence, it requires a higher temperature to obtain a satisfactory heat storage rate. However, the thermal conductivity of the original powder material is about 0.11 W/(m·K) [15], resulting in low heat transfer efficiency inside the reactor. Additionally, the water vapor pressure also has an undeniable impact on heat storage reaction rate. The low water vapor pressure corresponds to the low equilibrium temperature, which is beneficial for accelerating the heat storage reaction. Therefore, the water vapor, which is the product of the heat storage process, cannot accumulate in the reaction zone [16].

There are some measures to improve thermal conductivity for reference. For example, the thermal conductivity can be improved by compressing powder material due to a decrease in porosity. However, this method seems inappropriate for $Ca(OH)_2$/CaO. The compressed material is easy to break due to the volume expansion caused by the hydration process [17,18]. Furthermore, excessive compression is undesirable due to adverse effects on water vapor transport. Huang et al. [19] reported that an optional method is doping HBN. The thermal conductivity of heat storage material improves owing to the high thermal conductivity of doped material. Yan and Zhao [20,21] doped Li into pure $Ca(OH)_2$, and their experimental results in a fixed bed indicate that the heat storage rate is faster than pure material, which is mainly due to the reduction in energy barriers of heat storage reaction from 0.4 to 0.11 eV. The fixed bed, which is one of the relatively simple reactor types, is a heat storage process that has been widely studied in recent years. The heat storage material stays in the fixed reactor, and the heat from the external heat source can be transferred to the internal material through the wall of the heat exchange tube [22]. In this regard, the internal heat transfer performance is particularly important. The heat transfer from the heat sources to internal material is inefficient, and thus the heat storage reaction in the internal zone is incomplete. Although uniform heat transfer is also difficult to achieve due to the difference in thermal conductivity between zones with and without a fin, setting up fins is still feasible to improve the unfavorable heat transfer [23]. Chen et al. [24] utilized topology optimization algorithms to obtain a more optimized solution for fin setting. Although the shape of their fins is complex, the heat storage time can decrease by 43%. Wang et al. [25] proposed a fixed-bed reactor with a porous channel, which can improve heat transfer and promote the discharge of water vapor, leading to an accelerated heat storage reaction. Besides that, improving the structure of the fixed bed is another option. For instance, setting up the internal heating tube instead of the outside heating wall can shorten the heat transfer distance, and thus it can improve heat storage rate [26,27]. The heat storage material can be placed in multiple thin tubes, which can indirectly exchange heat with heat transfer fluid, and this shell–tube reactor has been proven to be feasible [28,29].

In a word, the structure of the fixed bed is relatively simple compared to the fluidized or moving bed, and its internal heat transfer needs to be improved. Setting up fins is a feasible and simple solution to this issue. This paper aims at the improvement of heat storage performance in the fixed bed by the Y-shaped fin. At present, although the feasibility

of using a Y-shaped fin for latent heat storage has been proved [30,31], its application to calcium hydroxide thermochemical heat storage. Therefore, this paper attempts to prove its feasibility by comparing performance inside the fixed bed without a fin, with a Y-shaped fin, and with a regular rectangle fin.

2. Models

2.1. Physical Model

Figure 1 shows the schematic diagram of the reactor structure. The heat storage process in a reactor with a diameter d1 of 200 mm is studied in this paper. The internal heating tube with a diameter d2 of 50 mm is set in the middle position, and four exhaust pipes with a diameter d3 of 20 mm are evenly arranged between the heating tube and the outer wall of the reactor, which can be used to discharge the water vapor generated by the dehydration reaction. For simplicity, the reactor is modeled as a two-dimensional system in the subsequent simulations. As shown in Figure 1b,c, four rectangular or Y-shaped fins are evenly arranged around the heating tube. The width of these fins is 1 mm, and the length of the rectangular fin $L1$ is equal to the distance between the heating tube and the outer wall of the reactor. As shown in Figure 1c, the Y-shaped fins are composed of two parts with the length of $L2$ and $L3$, and the angle at the top is α. It is important to note that the total length of both the rectangular and Y-shaped fins is equivalent, as described in Equation (2). Consequently, the total amount of thermal storage material in reactors with either fin configuration remains the same.

$$L2 + 2L3 = L1 \tag{2}$$

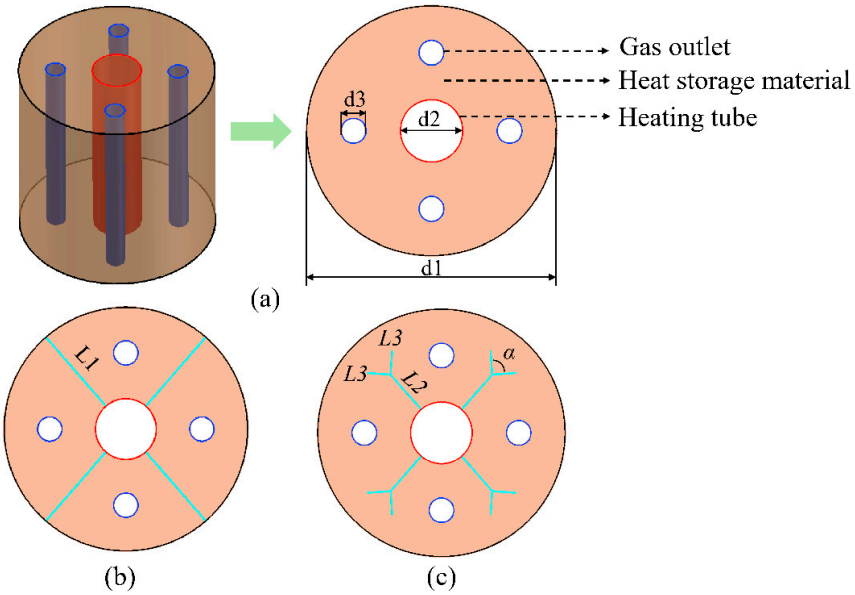

Figure 1. Schematic diagram of reactor structure: (**a**) without fin; (**b**) rectangular fin; (**c**) Y-shaped fin.

2.2. Numerical Model

In this paper, in addition to using a two-dimensional simplified model, some other simplification treatments are also carried out [32,33]. That is, the outer wall of the reactor is well insulated, and thus the heat transfer to the surrounding environment is not considered. The variations in particle size and porosity of heat storage material during the reaction are not considered, and the heat storage material is a continuous porous media. The gas is treated as an ideal gas, and it is in thermal equilibrium with the particles, and thus their temperatures are equal.

The governing equations of mass, momentum, and energy for gas are as follows:

$$\frac{\partial(\varepsilon\rho_g)}{\partial t} + \nabla \cdot (\rho_g u) = S_M \tag{3}$$

$$\frac{\partial(\rho_g u)}{\partial t} + \frac{u}{\varepsilon} \cdot \nabla(\rho_g u) = -\varepsilon\nabla P + \mu_g \nabla^2 u + F \tag{4}$$

$$\frac{\partial((\rho c_p)_{eff} T)}{\partial t} + u \cdot \nabla\left((\rho c_p)_g T\right) = \nabla\left(\lambda_{eff}\nabla T\right) + S_Q \tag{5}$$

where t is time, s; u is the velocity of gas, m/s; ρ_g is the density of gas, kg/m^3; ε is the porosity of heat storage material; μ_g is the dynamic viscosity of gas, Pa·s; T is the temperature, K. S_M and S_Q are the variation in mass and energy of gas caused by the reaction, kg/(m^3·s) and W/m^3, respectively. F is the flow resistance of gas, N/m^3. $(\rho c_p)_{eff}$ and λ_{eff} is the effective volumetric heat capacity and the effective thermal conductivity in the porous zone.

The dehydration process of $Ca(OH)_2$ is related to heat and mass transfer, which can refer to the relationship between equilibrium temperature and equilibrium pressure. When the temperature is higher than the equilibrium temperature corresponding to the current pressure, the dehydration reaction can proceed. The relationship between equilibrium temperature and equilibrium pressure is calculated by Equation (6) [34,35].

$$\ln\left(\frac{P_{eq}}{10^5}\right) = 16.508 - \frac{12845}{T_{eq}} \tag{6}$$

where the P_{eq} is the equilibrium pressure, Pa; the T_{eq} is the equilibrium temperature, K.

The dehydration reaction rate can be calculated by [34]

$$\frac{dX}{dt} = A\exp\left(-\frac{E}{\mathrm{Rg}T}\right)\left(\frac{T}{T_{eq}} - 1\right)(1 - X) \tag{7}$$

where X is the reaction extent; A represents the pre-exponential factor of dehydration; E represents the activation energy; Rg is the gas constant, J/(mol·K).

The concentration of reactant can be calculated by

$$\frac{dC_R}{dt} = -C_R\frac{dX}{dt} \tag{8}$$

The above parameters in the governing equations of gas are given as follows:

$$S_M = M_w C_R \frac{dX}{dt} \tag{9}$$

$$S_Q = -C_R\frac{dX}{dt}\Delta H \tag{10}$$

$$F = -\frac{\mu_g 180(1-\varepsilon)^2}{{D_s}^2\varepsilon^3}u \tag{11}$$

$$(\rho c_p)_{eff} = \varepsilon\rho_g c_{p,g} + (1-\varepsilon)\rho_s c_{p,s} \tag{12}$$

$$\lambda_{eff} = \varepsilon\lambda_g + (1-\varepsilon)\lambda_s \tag{13}$$

$$\rho_s = (1-X)\rho_R + X\rho_{PR} \tag{14}$$

$$c_{p,s} = (1-X)c_{p,R} + Xc_{p,PR} \tag{15}$$

$$c_{p,R} = 0.3829T + 1218.87 \tag{16}$$

$$c_{p,PR} = 0.1634T + 799.15 \tag{17}$$

where C_R is the concentration of reactant ($Ca(OH)_2$), mol/m^3; λ_s is the thermal conductivity of heat storage material, W/(m·K); M_w is the mole mass of water vapor, kg/mol; D_s is the particle size, m. ρ_s is the density of heat storage material; ρ_R and ρ_{PR} are the density of the reactant and product (CaO), respectively, kg/m^3. $C_{p,s}$ is the specific heat of heat storage material; $C_{p,R}$ and $C_{p,PR}$ are the specific heat of the reactant and product, respectively, J/(kg·K).

The values of the main parameters are listed in Table 1.

Table 1. The values of the main parameters.

Subjects	Values	Subjects	Values
A	7.15×10^9 1/s	λ_s	2 W/(m·K)
E	1.87×10^5 J/mol	ρ_R	2200 kg/m^3
D_s	5 μm	ρ_{PR}	1665 kg/m^3

The initial temperature inside the reactor is set to 723 K, and the initial pressure is set to 28,415 Pa, which is the corresponding equilibrium pressure for the initial temperature. The outer wall of the reactor is modeled as an adiabatic boundary, while the four exhaust pipes are set as pressure outlet boundaries with a pressure of 28,415 Pa. For the base case, the wall temperature of the heating tube is 873 K, the porosity of the heat storage material is 0.8, and the thermal conductivity of the fin is 45 W/(m·K). Additionally, the heat storage process is simulated by the COMSOL software.

To illustrate the availability of the present model, the grid independence analysis and the accuracy verification are studied, and the results are shown in Figure 2. It can be seen from the results that with the increase in the number of cells, the reaction time will remain stable at a certain value. To reduce computation time, the grid with a cell number of 4290 is selected for the reactor without a fin, while the cell numbers are 15,968 and 15,800 for the reactor with the Y-shaped fin and rectangular fin, respectively. Furthermore, Chen et al. [24] studied the heat storage process of a fixed-bed reactor, and the present model is validated by comparison with it. Due to the similar physical process, the governing equations of the present model can be used to simulate the heat storage process in the literature. The physical model identical to the literature is established using the present modeling method, and the results of the present model and literature are similar; thus, the present model is verified. Additionally, in our previous paper [27], the model is validated by comparing it with a fixed-bed experiment.

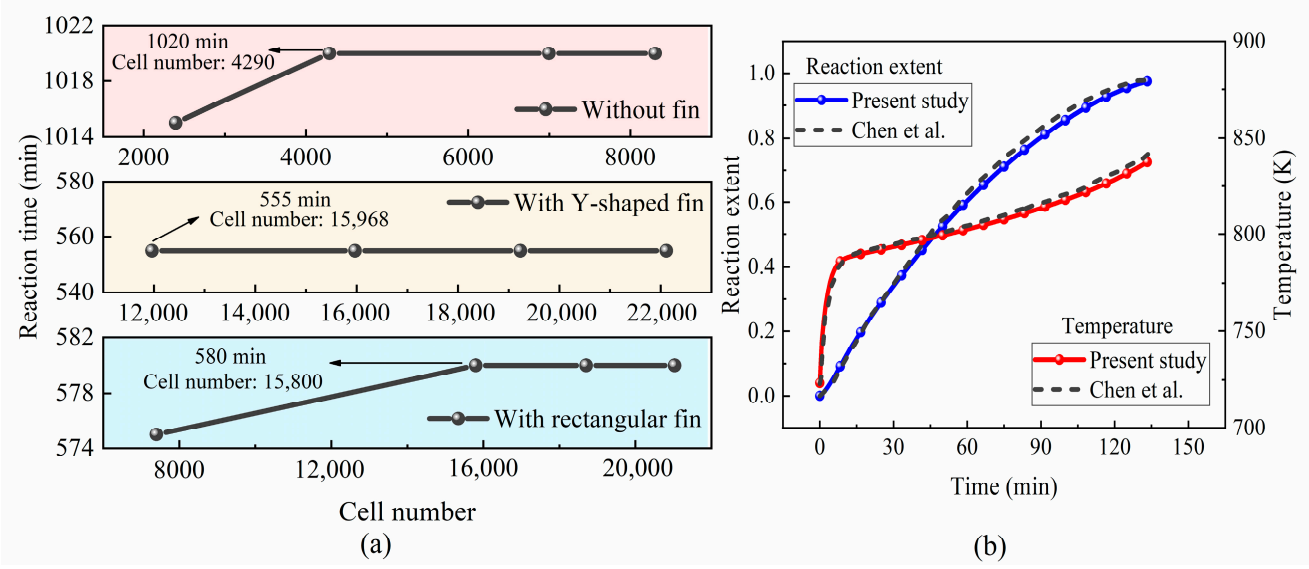

Figure 2. Model validation: (**a**) grid independence; (**b**) accuracy [24].

3. Results and Discussion

3.1. Effects of Fin Setting

The parameters *L*2, *L*3, and α can affect the configuration of the Y-shaped fin, thereby affecting the heat storage temperature. Therefore, the effects of the Y-shaped fin setting are studied in this section. The α changes from 30° to 150° and the *L*2 is set to 18.75, 37.5, and 56.25 mm, respectively, while *L*3 can be obtained by Equation (2). Figure 3 shows the effects of the Y-shaped fin setting, and the reaction time, average temperature, average concentration of reactant, and average pressure inside the reactor are used to evaluate the heat storage performance. As shown in Figure 3a, as *L*2 increases, the influence of α on heat storage time diminishes. When *L*2 is 56.25 mm, the heat storage time is 575 min at different α. However, when *L*2 is 18.75 mm, there is a significant difference in heat storage time for the cases with different α. The heat storage time is 555 min when α is 90°, which is the minimum among the cases studied in this paper. The heat storage time increases to 620 min when α is 150°, which is the maximum among the cases studied in this paper. As shown in Figure 3c,d, the temperature and concentration of reactant in these cases are similar at the initial stage, which indicates that the reaction rates of these cases are also similar. The heat storage reaction can generate water vapor, leading to an increase in pressure. However, when *L*2 is 18.75 mm and α is 150°, the pressure of this case is the minimum at the initial stage. This could be attributed to the fact that the water vapor generated in the reaction area is more likely to escape during the initial stage. As the reaction progresses, the increase in temperature of the case with *L*2 at 18.75 mm and α at 150° is slow compared to other cases. As a result, its heat storage reaction rate slows down, and its pressure becomes the maximum value among these cases due to a large amount of remaining reactants. Additionally, although the heat storage processes for most cases seem to be similar, the recommended setting scheme is *L*2 at 18.75 mm and α at 150°, which has the shortest reaction time among the setting schemes studied in this paper.

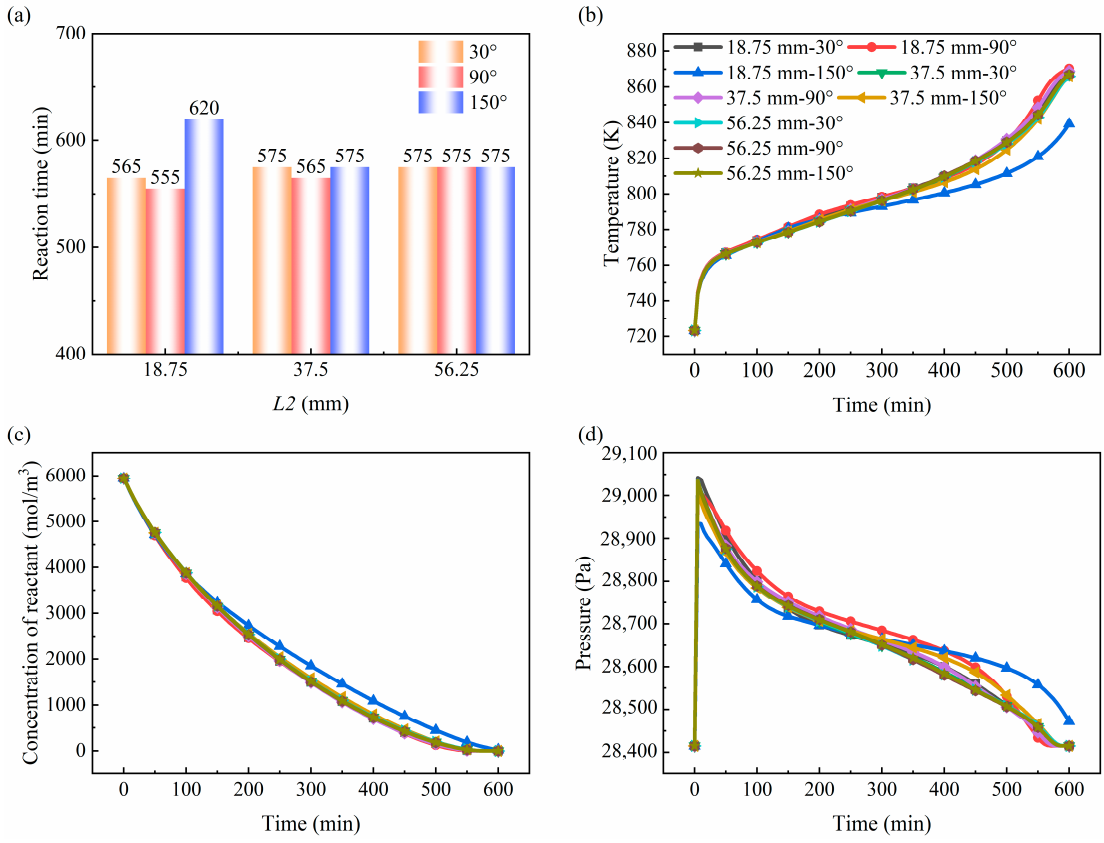

Figure 3. Effects of Y-shaped fin setting: (**a**) reaction time; (**b**) temperature; (**c**) concentration of reactant; (**d**) pressure.

To further demonstrate the feasibility of the Y-shaped fin, the heat storage performance of the reactor without a fin, with a rectangular fin, and with a Y-shaped fin is compared. Moreover, the Y-shaped fin with $L2$ at 18.75 mm and α at 150°, which has the shortest reaction time, is used for subsequent research, and Figure 4 shows the comparison results. It can be seen that the fin can effectively improve heat storage performance, and the Y-shaped fin shows a greater improvement. The heat storage time with the rectangular fin can decrease by 43.14% compared to the reactor without a fin. Setting a Y-shaped fin can further reduce heat storage time by 4.31% compared to the reactor with a rectangular fin, which decreases by 45.59% compared to the reactor without a fin. This is mainly attributed to the thermal conductivity of the fin. As shown in Figure 4c, the temperature inside the reactor without a fin slowly increases, while the temperature inside the reactor with a rectangular fin or Y-shaped fin is higher. Furthermore, the reactor with a Y-shaped fin shows slightly better heat transfer performance, and thus its temperature is slightly higher than that of a rectangular fin. And the trend of temperature change is the same for both. Due to the endothermic reaction, the trend of temperature increase is relatively small at the initial stage. Afterward, as the reaction approaches completion, the temperature rapidly increases. Therefore, the higher temperature in the reactor with the Y-shaped fin results in a slightly faster heat storage rate. As shown in Figure 4b,d, the consumption of reactant is slightly higher inside the reactor with a Y-shaped fin, which leads to the production of more water vapor, causing an increase in pressure.

Further, the size of the heating tube is an important parameter, which has a significant impact on heat transfer and heat storage capacity. That is, a larger size is beneficial for heat transfer, but it reduces heat storage capacity. Hence, the comparison results of the reactor equipped with heating tubes of different sizes for the rectangular fin and Y-shaped fin are shown in Figure 4e. It can be found that the heat storage rate in the reactor with a Y-shaped fin is faster than that in the reactor with a rectangular fin when the reactor is equipped with heating tubes of different sizes. Moreover, with the decrease in size of the heating tube, the difference between the two types of fins becomes more pronounced. When the radius of the heating tube is 12.5 mm, the heat storage time of the Y-shaped fin decreases by 4.76% compared to the rectangular fin. This improvement in heat storage time decreases by 2.99% when the radius of the heating tube is 50 mm. Therefore, the Y-shaped fin has superior heat storage performance, especially in the reactor equipped with a smaller-sized heating tube, which can provide more heat storage capacity.

To further compare the heat storage process of the reactor without a fin, with a Y-shaped fin, and with a rectangular fin, the temperature, reaction extent, and pressure fields inside the reactor are compared, and the distribution patterns are shown in Figures 5–7. It can be seen from Figure 5 that since the heat is gradually transferred from the middle heating tube to the surrounding area and the thermal conductivity of heat storage material is low, only the middle area has a higher temperature when the reactor has no fin. The temperature around the fin increases when the reactor is equipped with a rectangular or Y-shaped fin, and thus the area of the high-temperature zone can be increased. Due to the larger influence area of the Y-shaped fin, it has more high-temperature areas compared to the rectangular fin, which becomes more apparent as the reaction approaches completion. In addition, the reaction extent distribution inside the reactor is related to the temperature distribution. That is to say, the reaction extent in the high-temperature zone is greater, which indicates that the heat storage rate is mainly determined by temperature. It can be found that the pressure inside the reactor is mainly affected by the water vapor generated by the heat storage reaction. As the reaction approaches completion and produces less water vapor, the pressure in the middle position gradually decreases, and this phenomenon is the same in all three reactors. However, due to the accelerated reaction, the pressure near the outside of the reactor is higher when setting the Y-shaped fin. High pressure often means a high equilibrium temperature, which is not conducive to accelerating the heat storage reaction. Fortunately, the fin enhances the heat transfer, and the increased temperature still accelerates the reaction.

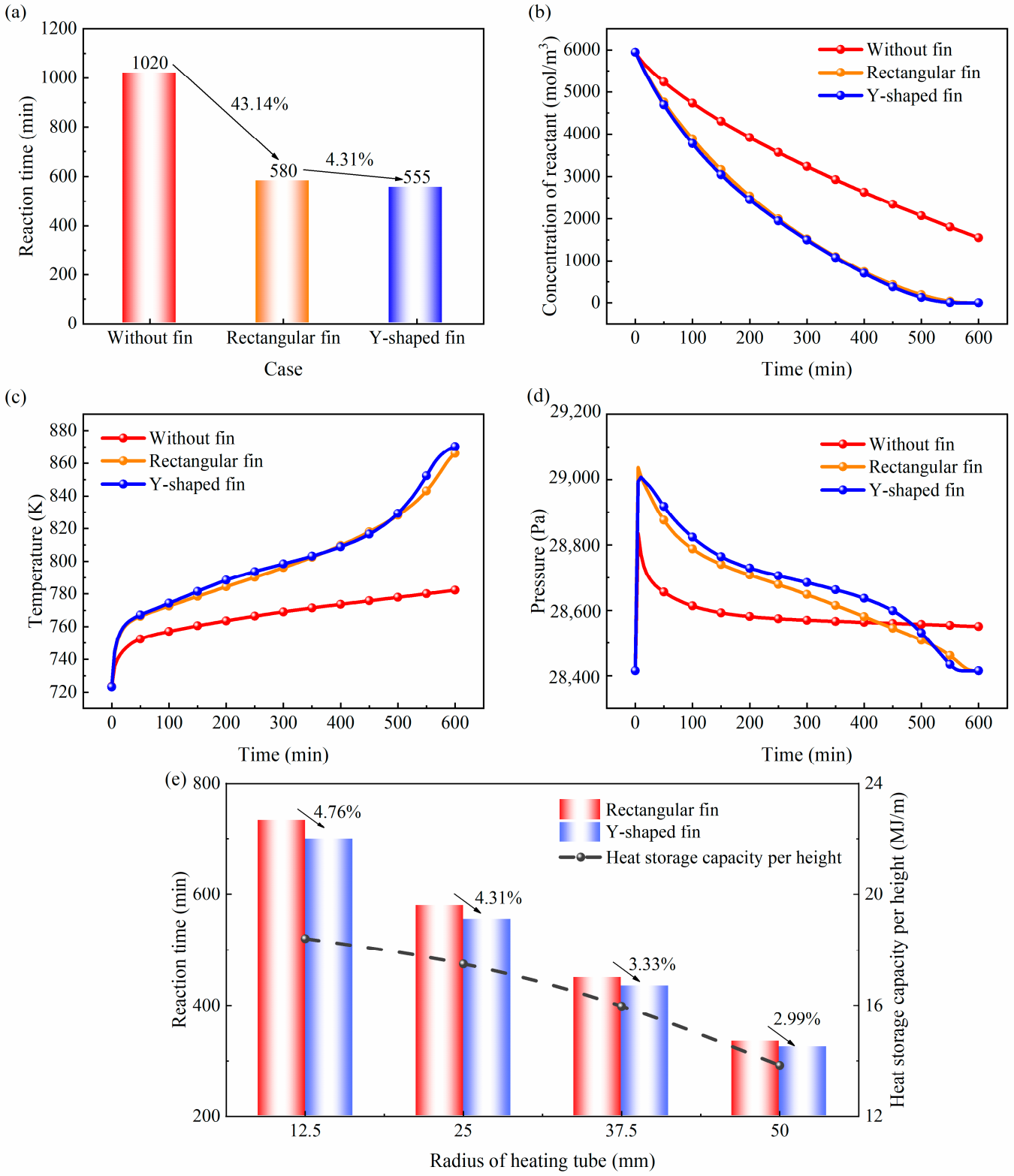

Figure 4. Comparison of without fin, rectangular fin, and Y-shaped fin: (**a**) reaction time; (**b**) concentration of reactant; (**c**) temperature; (**d**) pressure; (**e**) reaction time and heat capacity under different heating tube size.

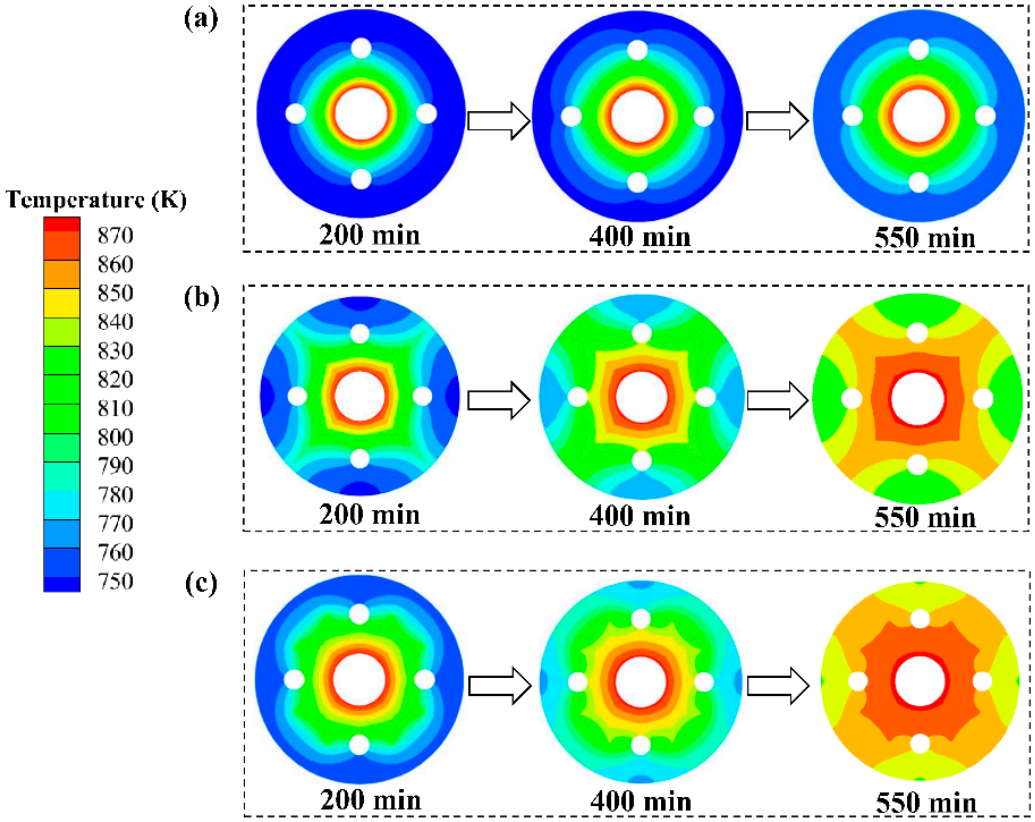

Figure 5. Comparison of temperature distribution: (**a**) without fin; (**b**) rectangular fin; (**c**) Y-shaped fin.

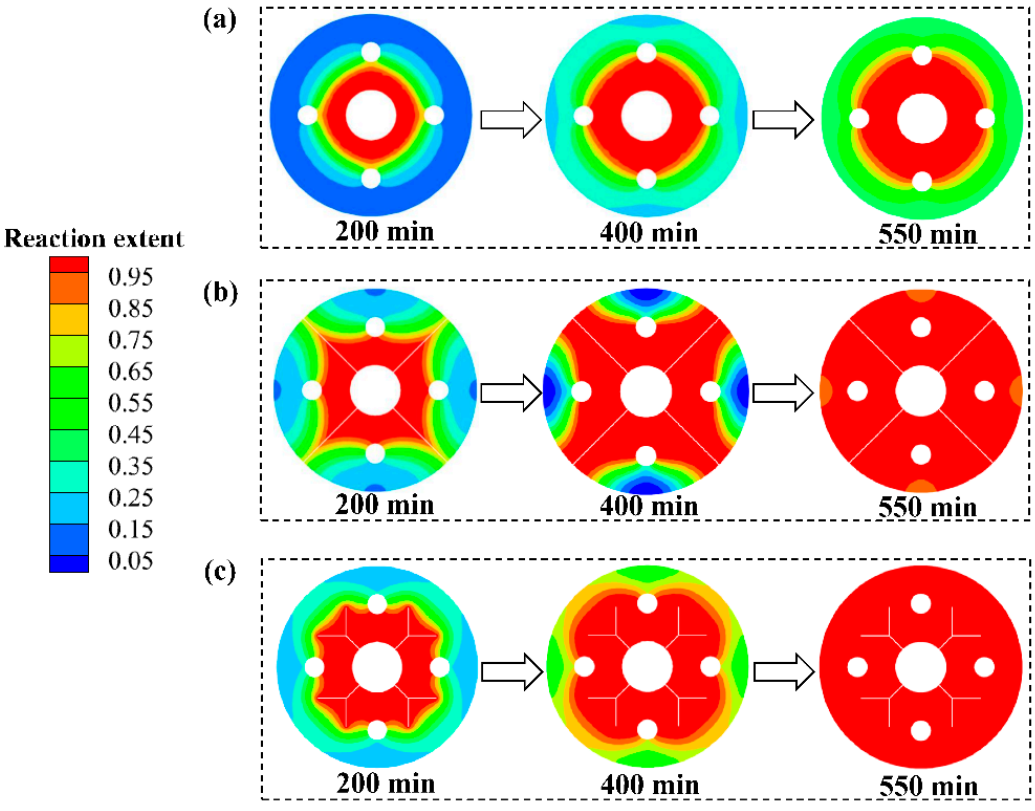

Figure 6. Comparison of reaction extent distribution: (**a**) without fin; (**b**) rectangular fin; (**c**) Y-shaped fin.

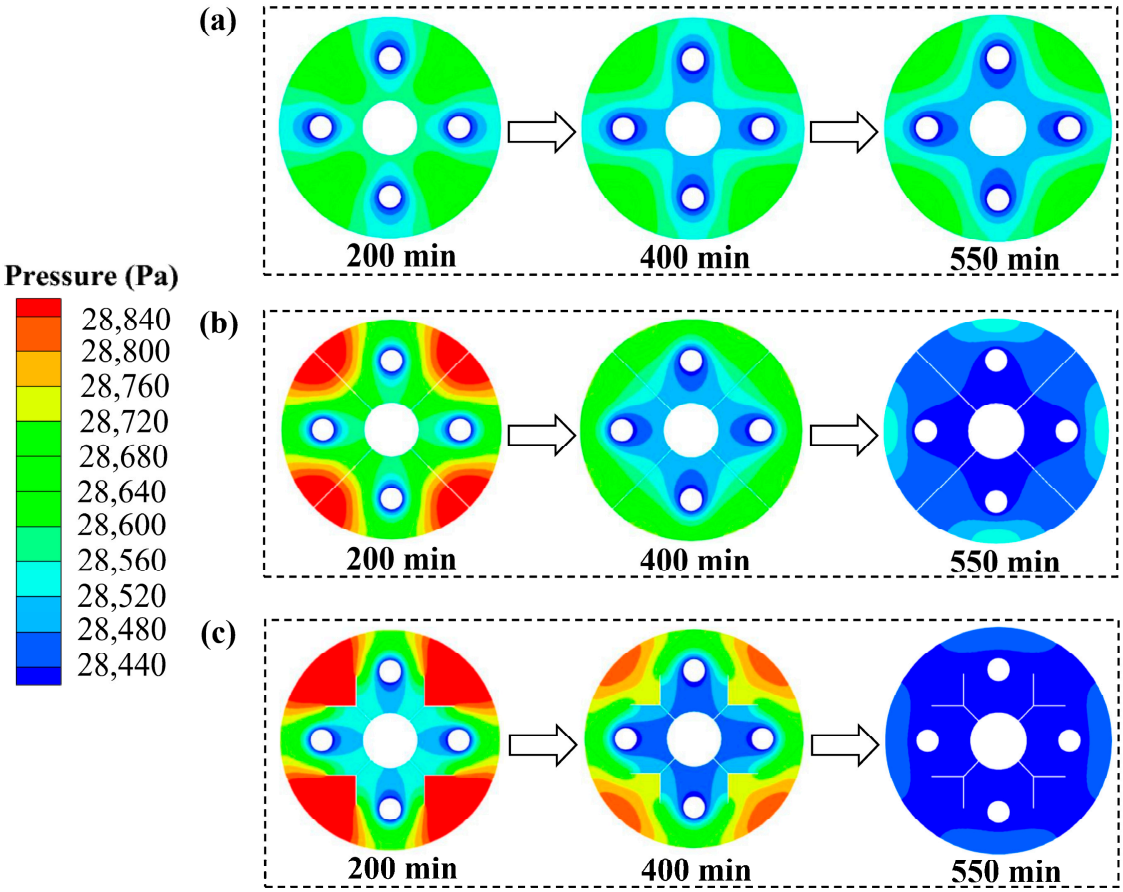

Figure 7. Comparison of pressure distribution: (**a**) without fin; (**b**) rectangular fin; (**c**) Y-shaped fin.

3.2. Performance Analysis Under Different Operation Conditions

This section discusses the effects of several operating parameters, such as the wall temperature of the heating tube, the porosity of the heat storage material, and the thermal conductivity of the fin. To demonstrate the feasibility of the Y-shaped fin, the heat storage time of the Y-shaped fin and rectangular fin are compared. Additionally, some parameters such as average temperature and concentration of reactant inside the reactor are used to evaluate the variation in the heat storage process for the reactor with the Y-shaped fin.

3.2.1. Wall Temperature of Heating Tube

The wall temperature of the heating tube is a key factor, which drives the progress of the heat storage reaction. Hence, it is vital to analyze the influence of heat storage temperature. Figure 8 displays the effects of wall temperature on the heat storage performance for rectangular fins and Y-shaped fins. It can be seen from Figure 8 that with the increase in wall temperature, the heat storage time decreases, and the difference between the Y-shaped fin and the rectangular fin increases. The heat storage time of the Y-shaped fin decreases by 3.09% compared to the rectangular fin when the wall temperature is 823 K, while it can decrease by 5.95% when the wall temperature increases to 923 K. As a result, the reactor with the Y-shaped fin outperforms the rectangular fin at high wall temperatures. Additionally, it can be found from Figure 8b that the high wall temperature can significantly accelerate the heat storage reaction. The concentration of reactant exhibits a remarkable downward trend due to the rapid temperature rise at high wall temperatures.

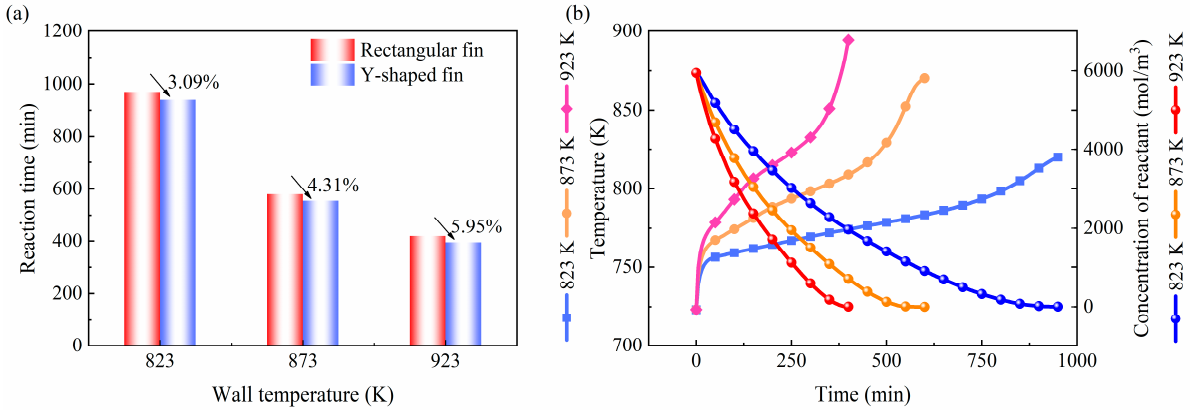

Figure 8. Effects of wall temperature: (**a**) comparison of reaction time between the rectangular and Y-shaped fin; (**b**) temperature and concentration of reactant of Y-shaped fin.

3.2.2. Porosity of Heat Storage Material

The porosity of the heat storage material is also worth considering, which affects the heat storage density and the flow of water vapor. Figure 9 shows the effects of the porosity of heat storage material. It can be seen from Figure 9a that with the increase in porosity of heat storage material, the heat storage time decreases due to the reduction in reactant. Moreover, for different porosities, the heat storage reaction of the Y-shaped fin is faster than that of the rectangular fin, indicating that the Y-shaped fin is superior. As shown in Figure 9b–d, the final heat capacity in the reactor decreases at high porosity, which also means that the heat absorption of the heat storage reaction decreases. Consequently, there is a noticeable upward trend in the temperature inside the reactor with high porosity. At high porosity, the water vapor produced by the dehydration reaction can readily escape; also, less water vapor is produced, which lowers the pressure inside the reactor.

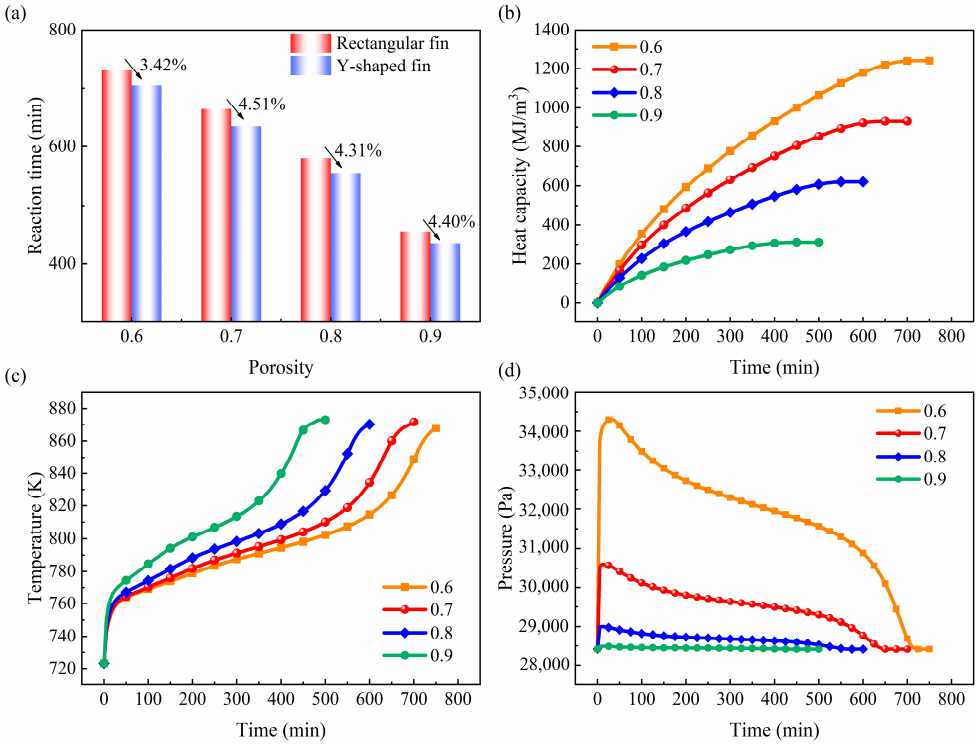

Figure 9. Effects of porosity: (**a**) comparison of reaction time between the rectangular and Y-shaped fin; (**b**) heat capacity of Y-shaped fin; (**c**) temperature of Y-shaped fin; (**d**) pressure of Y-shaped fin.

3.2.3. Thermal Conductivity of Fin

As mentioned above, the fin can enhance the heat transfer performance due to its relatively high thermal conductivity. Hence, it is also necessary to study the effects of the thermal conductivity of the fin on the heat storage process, and the results are shown in Figure 10. It can be found from Figure 10a that the heat storage time for both the Y-shaped fin and rectangular fin is reduced. Furthermore, the Y-shaped fin has a quicker heat storage reaction than the rectangular fin. When the thermal conductivity of the fin is 45 W/(m·K), the heat storage time of the Y-shaped fin decreases by 4.31% compared to the rectangular fin. It decreases by 8.05% when the thermal conductivity of the fin increases to 180 W/(m·K). Additionally, it can be seen from Figure 10b that the temperature inside the reactor with the Y-shaped fin presents a greater increasing trend at high thermal conductivity, resulting in a greater decrease in reactant concentration.

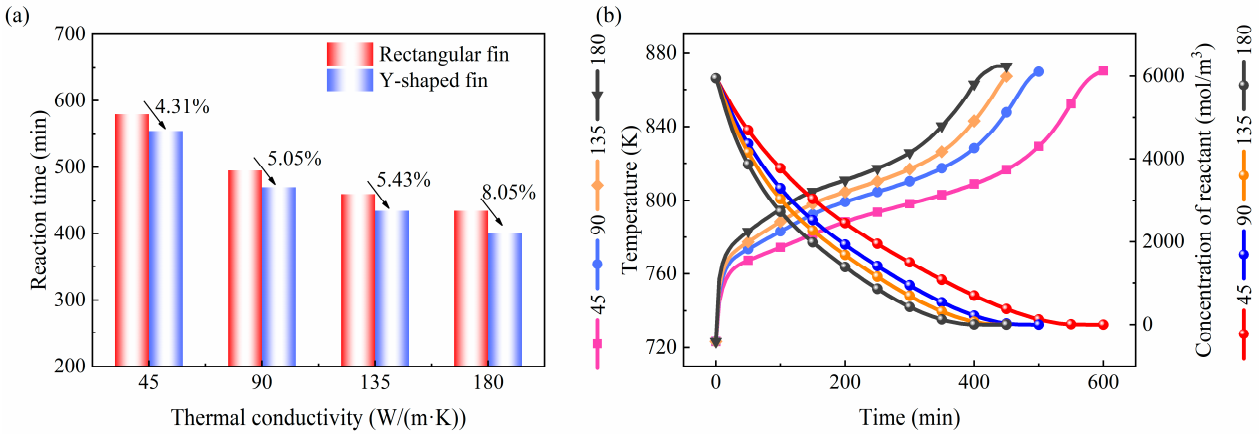

Figure 10. Effects of thermal conductivity of fin: (**a**) comparison of reaction time between the rectangular and Y-shaped fin; (**b**) temperature and concentration of reactant of Y-shaped fin.

4. Conclusions

In this paper, the heat storage performance of calcium hydroxide in a fixed-bed reactor is enhanced by the Y-shaped fin. A multi-physics numerical model is established for the heat storage process in the fixed bed. The layout of the Y-shaped fin is studied using the present model, which can obtain an optimized setting. The heat storage performance of the reactor with the Y-shaped fin, rectangular fin, and without fin are compared. Additionally, the effects of the main operation conditions on performance are also studied. The main results are as follows:

(1) The effects of the configuration of the Y-shaped fin on heat storage performance are not negligible. The top angle (α) has a minor impact on heat storage performance when the straight part ($L2$) is longer, while it has a significant impact when $L2$ is shorter. The recommended scheme is $L2$ at 18.75 mm and α at 150°. Both the rectangular fin and Y-shaped fin can improve heat storage performance, while the Y-shaped fin has a better improvement effect due to better heat transfer. Compared to the reactor without a fin, the heat storage time of the reactor with the rectangular fin decreases by 43.14%, and it can decrease by 45.59% for the reactor with the Y-shaped fin.

(2) The increase in wall temperature of the heating tube can significantly improve heat storage performance, and the reactor with the Y-shaped fin shows more performance improvement than the rectangular fin at high wall temperature. The heat storage time of the Y-shaped fin decreases by 3.09% compared to the rectangular fin when the wall temperature is 823 K, which decreases by 5.95% when the wall temperature is 923 K.

(3) The increase in porosity of heat storage material can shorten heat storage time due to the reduction in reactant, and the heat storage performance of the Y-shaped fin is still better than that of the rectangular fin at different porosity levels.

(4) With the increase in thermal conductivity of the fin, the heat storage performance is enhanced, and the reactor with the Y-shaped fin shows more performance improvement than the rectangular fin at high thermal conductivity. The heat storage time of the Y-shaped fin decreases by 4.31% compared to the rectangular fin when the thermal conductivity of the fin is 45 W/(m·K), while it decreases by 8.05% when the thermal conductivity of the fin is 180 W/(m·K).

In brief, due to the improved heat transfer, the Y-shaped fin is feasible for application in the fixed bed. To achieve a satisfactory performance, the number of Y-shaped fins may also need to be increased as the reactor size increases, which will decrease the heat storage capacity. Therefore, balancing heat storage capacity and storage time also needs to be considered for large-scale applications.

Author Contributions: Conceptualization, J.Y. (Jun Yan); Investigation, G.Z., Z.L., J.Y. (Jiakang Yao), Z.Z., S.Z., N.C. and L.J.; Methodology, L.J.; Project administration, G.Z., Z.L. and J.Y. (Jun Yan); Supervision, J.Y. (Jun Yan); Writing—original draft, L.J.; Writing—review and editing, J.Y. (Jun Yan) All authors have read and agreed to the published version of the manuscript.

Funding: This research is funded by the Science and Technology Project of State Grid of China with fund number 5419-202258359A-2-0-HW.

Data Availability Statement: The original contributions presented in the study are included in the article, further inquiries can be directed to the corresponding author.

Conflicts of Interest: Authors Guangyao Zhao, Zhen Li, Jiakang Yao, Zhehui Zhao, Sixing Zhang and Na Cheng were employed by the company China Electric Power Research Institute. The remaining authors declare that the research was conducted in the absence of any commercial or financial relationships that could be construed as a potential conflict of interest.

References

1. Shen, M.; Kong, F.; Tong, L.; Luo, Y.; Yin, S.; Liu, C.; Zhang, P.; Wang, L.; Chu, P.K.; Ding, Y. Carbon capture and storage (CCS): Development path based on carbon neutrality and economic policy. *Carbon Neutrality* **2022**, *1*, 37. [CrossRef]
2. Han, X.Y.; Wang, L.; Ling, H.S.; Ge, Z.W.; Lin, X.P.; Dai, X.J.; Chen, H.S. Critical review of thermochemical energy storage systems based on cobalt, manganese, and copper oxides. *Renew. Sustain. Energy Rev.* **2022**, *158*, 112076. [CrossRef]
3. Carrillo, A.J.; Gonzalez-Aguilar, J.; Romero, M.; Coronado, J.M. Solar Energy on Demand: A Review on High Temperature Thermochemical Heat Storage Systems and Materials. *Chem. Rev.* **2019**, *119*, 4777–4816. [CrossRef] [PubMed]
4. Palacios, A.; Barreneche, C.; Navarro, M.E.; Ding, Y. Thermal energy storage technologies for concentrated solar power—A review from a materials perspective. *Renew. Energ.* **2020**, *156*, 1244–1265. [CrossRef]
5. Alva, G.; Lin, Y.; Fang, G. An overview of thermal energy storage systems. *Energy* **2018**, *144*, 341–378. [CrossRef]
6. Yan, J.; Lu, L.; Ma, T.; Zhou, Y.; Zhao, C.Y. Thermal management of the waste energy of a stand-alone hybrid PV-wind-battery power system in Hong Kong. *Energ. Convers. Manag.* **2020**, *203*, 112261. [CrossRef]
7. Zhao, Y.; Zhao, C.Y.; Markides, C.N.; Wang, H.; Li, W. Medium- and high-temperature latent and thermochemical heat storage using metals and metallic compounds as heat storage media: A technical review. *Appl. Energ.* **2020**, *280*, 115950. [CrossRef]
8. Zhao, C.; Yan, J.; Tian, X.; Xue, X.; Zhao, Y. Progress in thermal energy storage technologies for achieving carbon neutrality. *Carbon Neutrality* **2023**, *2*, 10. [CrossRef]
9. Bellan, S.; Kodama, T.; Gokon, N.; Matsubara, K. A review on high-temperature thermochemical heat storage: Particle reactors and materials based on solid-gas reactions. *Wiley Interdiscip. Rev.-Energy Environ.* **2022**, *11*, e440. [CrossRef]
10. Wang, K.; Yan, T.; Li, R.K.; Pan, W.G. A review for $Ca(OH)_2$/CaO thermochemical energy storage systems. *J. Energy Storage* **2022**, *50*, 104612. [CrossRef]
11. Jiang, L.; Yan, J.; Tian, X.K.; Zhao, C.Y.; Fan, X. Thermochemical heat storage and material behavior of calcium hydroxide fine powder in a fluidized bed reactor. *Energy* **2024**, *312*, 133691. [CrossRef]
12. Bayon, A.; Bader, R.; Jafarian, M.; Fedunik-Hofman, L.; Sun, Y.; Hinkley, J.; Miller, S.; Lipiński, W. Techno-economic assessment of solid–gas thermochemical energy storage systems for solar thermal power applications. *Energy* **2018**, *149*, 473–484. [CrossRef]
13. Jiang, L.; Yan, J.; Tian, X.K.; Zhao, C.Y. Performance evaluation of ZTA ceramic encapsulated calcium hydroxide pellets for thermochemical heat storage. *J. Energy Storage* **2024**, *84*, 110888. [CrossRef]
14. Sole, A.; Martorell, I.; Cabeza, L.F. State of the art on gas-solid thermochemical energy storage systems and reactors for building applications. *Renew. Sustain. Energy Rev.* **2015**, *47*, 386–398. [CrossRef]
15. Afflerbach, S.; Kappes, M.; Gipperich, A.; Trettin, R.; Krumm, W. Semipermeable encapsulation of calcium hydroxide for thermochemical heat storage solutions. *Sol. Energy* **2017**, *148*, 1–11. [CrossRef]

16. Ye, H.; Tao, Y.B.; Wu, Z.H. Performance improvement of packed bed thermochemical heat storage by enhancing heat transfer and vapor transmission. *Appl. Energ.* **2022**, *326*, 119946. [CrossRef]
17. Fujii, I.; Ishino, M.; Akiyama, S.; Murthy, M.S.; Rajanandam, K.S. Behavior of $Ca(OH)_2$/CaO pellet under dehydration and hydration. *Sol. Energy* **1994**, *53*, 329–341. [CrossRef]
18. Briones, L.; Valverde-Pizarro, C.M.; Barras-Garcia, I.; Tajuelo, C.; Sanz-Perez, E.S.; Sanz, R.; Escola, J.M.; Gonzalez-Aguilar, J.; Romero, M. Development of stable porous silica-coated $Ca(OH)_2/\gamma$-Al_2O_3 pellets for dehydration/hydration cycles with application in thermochemical heat storage. *J. Energy Storage* **2022**, *51*, 104548. [CrossRef]
19. Huang, C.; Xu, M.; Huai, X. Experimental investigation on thermodynamic and kinetic of calcium hydroxide dehydration with hexagonal boron nitride doping for thermochemical energy storage. *Chem. Eng. Sci.* **2019**, *206*, 518–526. [CrossRef]
20. Yan, J.; Zhao, C.Y. First-principle study of CaO/$Ca(OH)_2$ thermochemical energy storage system by Li or Mg cation doping. *Chem. Eng. Sci.* **2014**, *117*, 293–300. [CrossRef]
21. Yan, J.; Zhao, C.Y. Experimental study of CaO/$Ca(OH)_2$ in a fixed-bed reactor for thermochemical heat storage. *Appl. Energ.* **2016**, *175*, 277–284. [CrossRef]
22. Almendros-Ibanez, J.A.; Fernandez-Torrijos, M.; Diaz-Heras, M.; Belmonte, J.F.; Sobrino, C. A review of solar thermal energy storage in beds of particles: Packed and fluidized beds. *Sol. Energy* **2019**, *192*, 193–237. [CrossRef]
23. Pan, Z.H.; Zhao, C.Y. Gas-solid thermochemical heat storage reactors for high-temperature applications. *Energy* **2017**, *130*, 155–173. [CrossRef]
24. Chen, J.T.; Xia, B.Q.; Zhao, C.Y. Topology optimization for heat transfer enhancement in thermochemical heat storage. *Int. J. Heat. Mass. Tran.* **2020**, *154*, 119785. [CrossRef]
25. Wang, M.; Chen, L.; He, P.; Tao, W.-Q. Numerical study and enhancement of $Ca(OH)_2$/CaO dehydration process with porous channels embedded in reactors. *Energy* **2019**, *181*, 417–428. [CrossRef]
26. Liu, X.; Duan, L.; Zhu, Z.; Yu, K.; Yang, L.; Chen, B. Energy storage characteristics and size optimization of $Ca(OH)_2$/CaO reactor with the embedded heating tube bundle. *Appl. Therm. Eng.* **2023**, *221*, 119861. [CrossRef]
27. Yan, J.; Jiang, L.; Zhao, C. Numerical Simulation of the $Ca(OH)_2$/CaO Thermochemical Heat Storage Process in an Internal Heating Fixed-Bed Reactor. *Sustainability* **2023**, *15*, 7141. [CrossRef]
28. Wang, M.; Chen, L.; Zhou, Y.; Tao, W.-Q. Numerical simulation of the calcium hydroxide/calcium oxide system dehydration reaction in a shell-tube reactor. *Appl. Energ.* **2022**, *312*, 118778. [CrossRef]
29. Wang, W.; Shuai, Y.; Yang, J.; Lougou, B.G.; Huang, Y. Heat transfer and heat storage characteristics of calcium hydroxide/oxide based on shell-tube thermochemical energy storage device. *Renew. Energ.* **2023**, *218*, 119364. [CrossRef]
30. Abed, A.M.; Mouziraji, H.R.; Bakhshi, J.; Dulaimi, A.; Mohammed, H.I.; Ibrahem, R.K.; Ben Khedher, N.; Yaici, W.; Mahdi, J.M. Numerical analysis of the energy-storage performance of a PCM-based triplex-tube containment system equipped with arc-shaped fins. *Front. Chem.* **2022**, *10*, 1057196. [CrossRef]
31. Ben Khedher, N.; Togun, H.; Abed, A.M.; Al-Najjar, H.M.T.; Dulaimi, A.; Mohammed, H.I.; Mahdi, J.M.; Yvaz, A.; Talebizadehsardari, P. Discharge performance assessment of a vertical double-pipe latent heat storage unit equipped with circular Y-shaped fins. *J. Build. Eng.* **2023**, *75*, 106870. [CrossRef]
32. Schaube, F.; Utz, I.; Woerner, A.; Mueller-Steinhagen, H. De- and rehydration of $Ca(OH)_2$ in a reactor with direct heat transfer for thermo-chemical heat storage. Part B: Validation of model. *Chem. Eng. Res. Des.* **2013**, *91*, 865–873. [CrossRef]
33. Jiang, L.; Yan, J. A new reactor with porous baffle for thermochemical heat storage: Design and performance analysis. *Appl. Therm. Eng.* **2024**, *257*, 124253. [CrossRef]
34. Ranjha, Q.; Oztekin, A. Numerical analyses of three-dimensional fixed reaction bed for thermochemical energy storage. *Renew. Energ.* **2017**, *111*, 825–835. [CrossRef]
35. Schaube, F.; Koch, L.; Woerner, A.; Mueller-Steinhagen, H. A thermodynamic and kinetic study of the de-and rehydration of $Ca(OH)_2$ at high H_2O partial pressures for thermo-chemical heat storage. *Thermochim. Acta* **2012**, *538*, 9–20. [CrossRef]